

# PIDDosome-independent tumor suppression by Caspase-2

C Manzl<sup>1</sup>, L Peintner<sup>1</sup>, G Krumschnabel<sup>1</sup>, F Bock<sup>1</sup>, V Labi<sup>1,4</sup>, M Drach<sup>2</sup>, A Newbold<sup>3</sup>, R Johnstone<sup>3</sup> and Andreas Villunger<sup>\*1</sup>

The PIDDosome, a multiprotein complex constituted of the 'p53-induced protein with a death domain (PIDD), 'receptor-interacting protein (RIP)-associated ICH-1/CED-3 homologous protein with a death domain' (RAIDD) and pro-Caspase-2 has been defined as an activating platform for this apoptosis-related protease. PIDD has been implicated in p53-mediated cell death in response to DNA damage but also in DNA repair and nuclear factor kappa-light-chain enhancer (NF- $\kappa$ B) activation upon genotoxic stress, together with RIP-1 kinase and Nemo/IKK $\gamma$ . As all these cellular responses are critical for tumor suppression and deregulated expression of individual PIDDosome components has been noted in human cancer, we investigated their role in oncogenesis induced by DNA damage or oncogenic stress in gene-ablated mice. We observed that Pidd or Caspase-2 failed to suppress lymphoma formation triggered by  $\gamma$ -irradiation or 3-methylcholanthrene-driven fibrosarcoma development. In contrast, Caspase-2 showed tumor suppressive capacity in response to aberrant *c-Myc* expression, which did not rely on PIDD, the BH3-only protein Bid (BH3 interacting domain death agonist) or the death receptor ligand Trail (TNF-related apoptosis-inducing ligand), but associated with reduced rates of p53 loss and increased extranodal dissemination of tumor cells. In contrast, Pidd deficiency associated with abnormal M-phase progression and delayed disease onset, indicating that both proteins are differentially engaged upon oncogenic stress triggered by *c-Myc*, leading to opposing effects on tumor-free survival.

*Cell Death and Differentiation* (2012) 19, 1722–1732; doi:10.1038/cdd.2012.54; published online 18 May 2012

Most members of the Caspase family of proteases are involved in killing damaged, harmful or unwanted cells while others regulate inflammation or differentiation. Recent studies suggest that one member of this family, Caspase-2, may exert even directly opposing functions such as either killing or saving cells after DNA damage.<sup>1</sup>

Activation of Caspase-2 is coordinated by complex pre- or post-translational modifications of enzyme expression or function, respectively. These involve differential splicing or phosphorylation at several serine sites, translocation between subcellular compartments, and/or recruitment into different activation complexes.<sup>2,3</sup> Following identification of a putative activation platform for Caspase-2, called the PIDDosome (PIDD/RAIDD/Caspase-2), which supported its assumed role as an initiator caspase of apoptosis,<sup>4</sup> evidence was provided that it might also be involved in an Ataxia telangiectasia mutated (ATM)/Ataxia telangiectasia and Rad3-related protein (ATR)-dependent cell death pathway controlled by checkpoint kinase-1 (Chk1). There, Caspase-2 killing appears to occur independent from classical apoptosis regulators such as Caspase-3 or B-cell lymphoma 2 (Bcl-2).<sup>5</sup>

However, it remains unclear if Caspase-2 requires activation in the PIDDosome, or another putative activation platform, such as the death inducing signaling complex (DISC),<sup>6</sup> or none of the above, under such conditions.

In addition, evidence for Caspase-2 as a critical effector in p53-induced apoptosis, acting upstream of mitochondria in response to anticancer agents such as 5-fluorouracil has also been provided.<sup>1,7</sup> Caspase-2 also appears to account for the post-mitotic death of cancer cells upon G2/M checkpoint failure.<sup>8</sup> Consistent with a role for the PIDDosome in p53-induced cell death, PIDD overexpression facilitated Caspase-2 activation and apoptosis in response to DNA damage in HeLa cells<sup>4</sup> and RNA interference or antisense oligonucleotides targeting PIDD mRNA delayed cell death induced by overexpression of p53 in H1299 colon cancer<sup>9</sup> or K562 myelogenous leukemia cells, respectively.<sup>10</sup>

While all these *in-vitro* studies provided evidence of an apoptotic function of the Caspase-2 containing PIDDosome, targeting PIDD or RAIDD by siRNA in HCT-116 colon carcinoma cells,<sup>7</sup> as well as analysis of gene-targeted mice lacking *Pidd*<sup>11,12</sup> or *Raid1*,<sup>13</sup> failed to provide supportive

<sup>1</sup>Division of Developmental Immunology, BIOCENTER, Medical University Innsbruck, Innsbruck, Austria; <sup>2</sup>Institute of Pathology, Medical University Innsbruck, East Melbourne, Victoria, Australia and <sup>3</sup>Peter MacCallum Cancer Centre, East Melbourne, Victoria, Australia

\*Corresponding author: A Villunger, Division of Developmental Immunology, BIOCENTER, Medical University Innsbruck, Innrain 80-82, Innsbruck 6020, Austria. Tel: + 43 512 9003 70380; Fax: + 43 512 9003 73960; E-mail: andreas.villunger@i-med.ac.at

<sup>4</sup>Current address: Max-Delbrück Center for Molecular Medicine, Berlin-Buch, Germany.

**Keywords:** apoptosis; Caspase-2; PIDDosome; cancer

**Abbreviations:** PIDD, p53-induced protein with a death domain; RAIDD, receptor-interacting protein-associated ICH-1/CED-3 homologous protein with a death domain; NF- $\kappa$ B, nuclear factor kappa-light-chain enhancer; Nemo/IKK $\gamma$ , NF- $\kappa$ B essential modulator/nuclear factor kappa-B kinase subunit gamma; ATM, Ataxia telangiectasia mutated; ATR, Ataxia telangiectasia and Rad3-related protein; Bcl-2, B-cell lymphoma 2; DISC, death inducing signaling complex; MEF, mouse embryonic fibroblast; 3-MC, 3-methylcholanthrene; Bid, BH3 interacting domain death agonist; TRAIL, TNF-related apoptosis-inducing ligand; Mdm2, murine double minute; PI, propidium iodide; BrdU, Bromodeoxyuridine; 53BP-1, p53 binding protein 1; RIP-1, receptor-interacting serine/threonine-protein kinase 1; TNF, tumor necrosis factor; IL, interleukin

Received 7.10.11; revised 29.2.12; accepted 15.3.12; Edited by B Zhivotovsky; published online 18.5.12

evidence as normal cell death responses in mouse embryonic fibroblast (MEF), lymphocytes and oocytes in response to DNA damage were reported. Furthermore, conflicting observations regarding cell death resistance of neurons were made in two different Caspase-2 knockout strains generated<sup>14,15</sup> and combined deletion of Caspase-2 plus Caspase-9 in hematopoietic cells failed to reveal any redundancy between both initiator caspases in apoptosis induction.<sup>16</sup>

Regardless of a pro-death or pro-survival function of PIDD or Caspase-2, all mechanisms they seem to be involved in are highly relevant for tumorigenesis. Noteworthy, expression of Caspase-2, encoded on Chr. 7q in humans harboring a putative tumor suppressor, has been reported to be reduced in patients suffering from acute myeloid leukemia or acute juvenile lymphoblastic leukemia where it correlates with poor prognosis or treatment resistance, respectively. Reduced protein expression was also reported in mantle cell lymphoma as well as in solid tumors such as gastric cancer and metastasizing tumors of the brain.<sup>17</sup> Along that line, a possible tumor suppressor function of PIDD is also supported by a reported correlation between apoptotic index and its protein levels in oral squamous cell carcinoma patient samples.<sup>18</sup>

In line with a tumor suppressive role of the PIDDosome, E1A/Ras-transformed MEF lacking Caspase-2 showed increased colony formation potential in soft agar and accelerated tumor formation in xeno-transplant studies. Even more striking, when *Eμ-Myc* transgenic mice, predisposed for B-cell lymphomagenesis, were crossed with *Casp2*<sup>-/-</sup> mice, further acceleration of tumor formation was observed.<sup>19</sup> The molecular basis for the accelerated tumorigenesis in relation to PIDDosome formation, however, remains unresolved but proposed to be accounted for by a more general resistance of Caspase-2-deficient cells to oncogenic stress or DNA damage.<sup>19</sup> To address the role of PIDDosome formation in tumor suppression, we have investigated DNA damage-induced as well as oncogene-triggered tumor formation in *Pidd*-deficient mice and compared it with the effects observed in the absence of Caspase-2, or, where appropriate, *p53*.

## Results

**The PIDDosome fails to prevent tumor formation triggered in response to DNA damage.** Both PIDD and Caspase-2 have been repeatedly implicated in the cellular response to DNA damage. Hence, we triggered lymphomagenesis in *Pidd*- and *Caspase-2*-deficient mice by repeated exposure to low-dose  $\gamma$ -irradiation, a well-established *in-vivo* model of DNA damage-driven tumor formation.<sup>20</sup> Tumorigenesis in this model is accelerated by loss of *p53*<sup>21</sup> and hence appeared most suitable to study the tumor suppressor potential of the PIDDosome. Wild-type (wt) mice developed thymic lymphomas with a median survival of 181 days (d). Consistent with published results, loss of *p53* accelerated tumor formation (median survival 107 d,  $P < 0.0001$ ) but absence of *Pidd* or its putative downstream apoptosis effector, Caspase-2, had no such effect (median survival 202 d and 185 d, respectively) (Figure 1a).

To expand these observations into a different model system of DNA damage-driven tumorigenesis, we also challenged mice by intramuscular injection of 3-methylcholanthrene

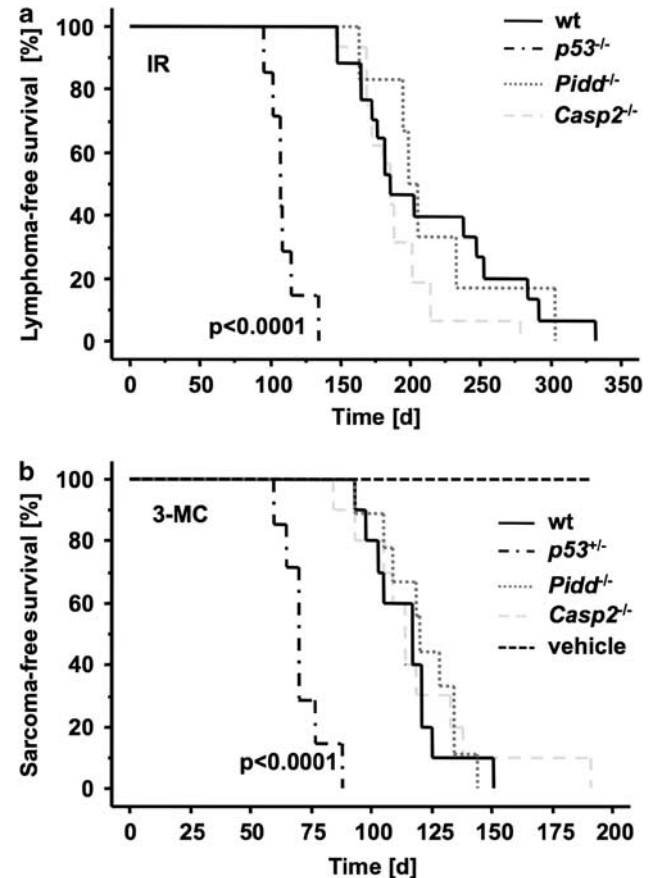


**Figure 1** Loss of *Pidd* or *Caspase-2* has no influence on DNA damage-induced tumorigenesis. (a) Tumor-free survival of wt ( $n = 18$ ), *Pidd*<sup>-/-</sup> ( $n = 6$ ) and *Casp2*<sup>-/-</sup> ( $n = 16$ ) mice after fractionated irradiation ( $4 \times 1.75$  Gy). No difference in the development of thymic lymphomas between the genotypes was observed. *P53*<sup>-/-</sup> mice ( $n = 7$ ) were included as positive controls, and earlier onset of thymic lymphomas was monitored ( $P < 0.0001$ ). (b) Tumor-free survival of wt ( $n = 11$ ), *Pidd*<sup>-/-</sup> ( $n = 10$ ), *Casp2*<sup>-/-</sup> ( $n = 11$ ) and *p53*<sup>+/-</sup> ( $n = 7$ ) mice after a single injection of 3-MC or vehicle (sesame oil;  $n = 7$ ) to induce fibrosarcomas. Sarcomas occurred significantly earlier in *p53*<sup>+/-</sup> animals compared with wt mice ( $P < 0.0001$ )

(3-MC), a carcinogen forming bulky adducts with DNA, leading to the formation of fibrosarcomas, again in a *p53*-regulated manner.<sup>22</sup> Consistently, loss of one allele of *p53* led to an accelerated onset of fibrosarcomas ( $P < 0.0001$ ), but loss of *Pidd* or *Caspase-2* had no such effect (Figure 1b).

Together, our results demonstrate that the PIDDosome is dispensable for tumor suppression in response to DNA-damage, inflicted by  $\gamma$ -irradiation or bulky-adduct formation.

**Loss of *Pidd* or *Caspase-2* deregulate *c-Myc*-induced lymphomagenesis.** To investigate if Caspase-2 depends on PIDDosome formation to suppress *c-Myc*-driven lymphomagenesis, *Casp2*<sup>-/-</sup> and *Pidd*<sup>-/-</sup> mice were intercrossed with mice overexpressing *c-Myc* under control of the Ig heavy chain enhancer, limiting expression of the transgene to the B-cell lineage.<sup>23</sup> Cohorts of wt *Eμ-Myc*, *Eμ-Myc/Pidd*<sup>-/-</sup> and *Eμ-Myc/Casp2*<sup>-/-</sup> mice were followed till development of disease. While *Eμ-Myc* mice (median survival 122 d) lacking Caspase-2 succumbed to disease significantly earlier

(median survival 90 d,  $P=0.0044$ ) and showed increased tumor burden in the spleen (Supplementary Figure S1),  $E\mu$ -Myc/*Pidd*<sup>-/-</sup> mice showed delayed onset of disease (median survival 250 d,  $P<0.0005$ ; Figure 2a). Immunophenotyping of lymphomas revealed that loss of Caspase-2 promoted mainly B-cell tumors of IgM<sup>+</sup> or mixed pre-B/IgM<sup>+</sup> phenotype (presented as IgM<sup>+/-</sup>) while early hematopoietic progenitor-derived lymphomas, represented as B220<sup>+</sup> CD4<sup>+</sup> tumors, were not observed so far in the absence of Caspase-2 ( $P=0.002$ ,  $\chi^2$ -test). Kaplan–Meier analysis confirmed that the altered latency in tumor-free survival observed in the absence of Caspase-2 was due to the faster rise of IgM<sup>+</sup> tumors ( $P=0.0028$ ; Figures 2b–d).

Previous reports suggested that the pro-apoptotic function of Caspase-2 relies in part in its capacity to process and activate the BH3-only pro-apoptotic Bcl-2 family protein BH3 interacting domain death agonist (Bid) into its active truncated form (tBid), upstream of mitochondrial outer membrane permeabilization,<sup>24</sup> and/or by sensitizing cells to Trail-mediated cell death by facilitating processing of pro-Caspase-8.<sup>25</sup> Therefore, we reasoned that impaired activation of Bid or ineffective Trail signaling may contribute to the accelerated tumor formation observed in Caspase-2-deficient mice overexpressing *c-Myc*. Hence, we also investigated cohorts of  $E\mu$ -Myc transgenic mice that lack Bid or Trail, but neither *Bid*<sup>-/-</sup> nor *Trail*<sup>-/-</sup> mice developed

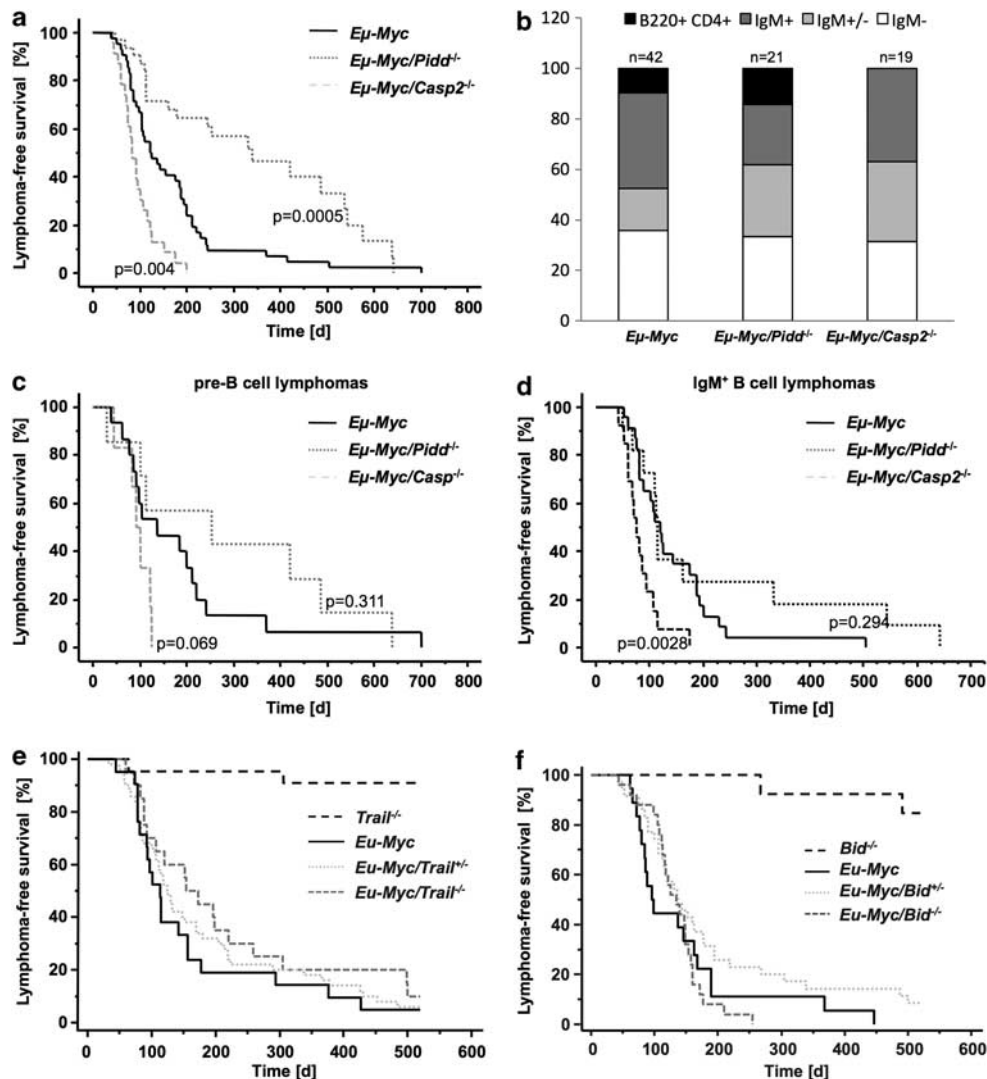


**Figure 2** Opposing effects of individual PIDDosome components on *c-Myc*-induced lymphomagenesis. (a) Cohorts of  $E\mu$ -Myc ( $n=42$ ),  $E\mu$ -Myc/*Pidd*<sup>-/-</sup> ( $n=41$ ) and  $E\mu$ -Myc/*Casp2*<sup>-/-</sup> ( $n=25$ ) mice were monitored for the development of B-cell lymphomas over time.  $E\mu$ -Myc mice lacking *Caspase-2* showed a significantly earlier onset of lymphomagenesis ( $P=0.0044$ ) compared with wt  $E\mu$ -Myc, while *Pidd* deficiency delayed lymphomagenesis in  $E\mu$ -mice ( $P=0.0005$ ). (b) Distribution of pro/pre-B (white), mixed IgM<sup>+/-</sup> (light gray), IgM<sup>+</sup> (dark gray) and B220<sup>+</sup> CD4<sup>+</sup> (black) lymphomas analyzed from mice of the indicated genotypes. The distribution of lymphomas in  $E\mu$ -Myc/*Casp2*<sup>-/-</sup> was significantly different ( $P=0.004$ ) compared with wt  $E\mu$ -Myc due to the higher amount of mixed and IgM<sup>+</sup> tumors. Kaplan–Meier analysis was depicted as (c) pre-B and (d) IgM<sup>+</sup> B lymphomas of indicated genotypes. In  $E\mu$ -Myc/*Casp2*<sup>-/-</sup> mice, IgM<sup>+</sup> tumors developed significantly earlier than in  $E\mu$ -Myc animals ( $P=0.0028$ ). (e) Kaplan–Meier analysis of *Bid*<sup>-/-</sup> ( $n=13$ ),  $E\mu$ -Myc (median survival 97 d,  $n=18$ ),  $E\mu$ -Myc/*Bid*<sup>+/-</sup> (median survival 137 d,  $n=35$ ) and  $E\mu$ -Myc/*Bid*<sup>-/-</sup> (median survival 134 d,  $n=25$ ) is shown. (f) Cohorts of *Trail*<sup>-/-</sup> ( $n=22$ ),  $E\mu$ -Myc (median survival 113 d,  $n=21$ ),  $E\mu$ -Myc/*Trail*<sup>+/-</sup> (median survival 125 d,  $n=50$ ) and  $E\mu$ -Myc/*Trail*<sup>-/-</sup> (median survival 164 d,  $n=20$ ) mice were monitored for the development of B-cell lymphomas over time

*E $\mu$ -Myc*-driven B-cell lymphomas earlier than *E $\mu$ -Myc* mice (Figures 2e and f).

Together, our findings demonstrate that Caspase-2-mediated suppression of *c-Myc*-driven lymphomagenesis does not depend on the formation of the PIDDosome, processing of its putative substrate Bid, or sensitization of cells to Trail-induced killing. Furthermore, Pidd appears to be able to exert oncogenic potential, most likely independent of its proposed Caspase-2 activating function.

**Caspase-2 deficiency reduces the pressure to lose p53.** Initially, the increased proliferative rate caused by *c-Myc* overexpression is balanced by massive apoptosis until counterselected for, for example, by inactivation of the ARF/murine double minute (Mdm2)/p53 signaling network.<sup>26</sup> Consistently, loss of alternative antagonists of *c-Myc*-driven lymphomagenesis, such as the pro-apoptotic BH3-only proteins Bim or Bmf, relieve the pressure to inactivate

p53 in *E $\mu$ -Myc* transgenic mice.<sup>27</sup> To monitor, if loss of *Caspase-2* also reduced the frequency of p53 inactivation, we performed western blot analysis for p53 and ARF, that can be used as markers for lost or mutated p53,<sup>26</sup> on primary tumor samples from *E $\mu$ -Myc*, *E $\mu$ -Myc/Pidd<sup>-/-</sup>* and *E $\mu$ -Myc/Casp2<sup>-/-</sup>* mice (Figure 3a). Our analysis revealed reduced p53 inactivation in the absence of Caspase-2 (2/21 cases; 9.5%), when compared with wt (9/40; 22.5%) or Pidd-deficient (4/17; 23.5%) *E $\mu$ -Myc* tumors. Moreover, Kaplan–Meier analysis of lymphomagenesis showed a significantly earlier tumor onset in *E $\mu$ -Myc/Casp2<sup>-/-</sup>* tumors ( $P < 0.0001$ ) with presumably normal p53 status (no immunoreactivity for ARF or p53 in western analysis) compared with wt *E $\mu$ -Myc* tumors while *E $\mu$ -Myc/Pidd<sup>-/-</sup>* lymphomas developed significantly later ( $P = 0.0291$ ) (Figure 3b, upper graph). In contrast, tumors carrying a mutation (immunoreactive for both ARF and p53) or a deletion of p53 (immunoreactivity for ARF but not for p53) showed no

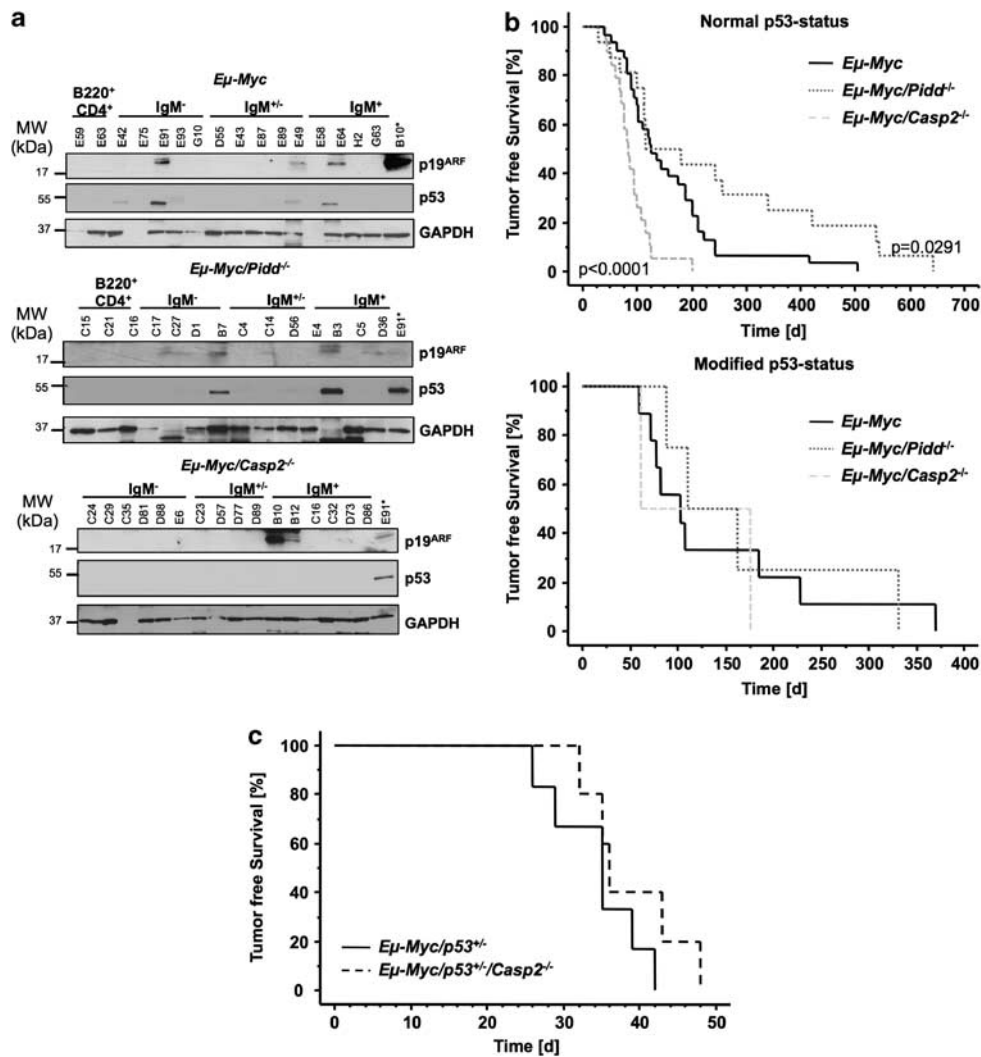


**Figure 3** Loss of *Caspase-2* relieves the pressure to lose p53. (a) Representative western blot analysis of p19<sup>ARF</sup> and p53 expression in tumors derived from *E $\mu$ -Myc*, *E $\mu$ -Myc/Pidd<sup>-/-</sup>* and *E $\mu$ -Myc/Casp2<sup>-/-</sup>*. GAPDH serves as a loading control. In the last lane, a lysate derived from *E $\mu$ -Myc/Casp2<sup>-/-</sup>* (B10) or *E $\mu$ -Myc* lymphoma (E91) is loaded as positive control. (b) Kaplan–Meier analysis of lymphomagenesis in mice with normal p53 or modified p53 status (mutated or lost, as assessed by western blotting in a). (c) Cohorts of *E $\mu$ -Myc/p53<sup>+/-</sup>* ( $n = 5$ ), and *E $\mu$ -Myc/p53<sup>+/-</sup>/Casp2<sup>-/-</sup>* ( $n = 5$ ) mice were monitored for the development of B-cell lymphomas over time and data are depicted as tumor-free survival in a Kaplan–Meier analysis

difference in latency between genotypes (Figure 3b, lower graph). These data suggest that Caspase-2 acts most likely in an alternative pathway, other than the ones activated by p53 upon oncogenic stress, or upstream of p53 itself. Yet, when Caspase-2 deficiency was combined with haplo-insufficiency for p53, no further acceleration of disease onset was observed, indicating that loss of heterozygosity that usually accelerates disease onset in  $E\mu$ -Myc/p53<sup>+/-</sup> mice is dominant over loss of Caspase-2 in  $E\mu$ -Myc-driven lymphomagenesis (Figure 3c).

**Normal cell death and proliferative responses in PIDDo-some-defective premalignant B cells.** As apoptosis defects are most critical in premalignant  $E\mu$ -Myc animals to allow *c-Myc*-driven transformation, we investigated if *Pidd* or *Caspase-2* loss may impact on *c-Myc*-mediated cell death and B-cell homeostasis in premalignant mice. Composition and distribution of different B-cell subsets in bone marrow, spleens and peripheral blood derived from premalignant  $E\mu$ -Myc/*Casp2*<sup>-/-</sup> mice showed no gross alterations, when compared with  $E\mu$ -Myc mice but loss of *Pidd* appeared to reduce the number of pre-B and immature T1 transitional B cells present in the spleen of transgenic animals ( $P=0.0584$  and  $P=0.0004$ , respectively; Figure 4a).

The reduced B-cell numbers may be due to increased rates of *c-Myc*-driven cell death or, alternatively, impaired proliferation in premalignant cells. Hence, pre-B as well as IgM<sup>+</sup>IgD<sup>-</sup> naive B cells were sorted from the bone marrow and spleen from wt  $E\mu$ -Myc,  $E\mu$ -Myc/*Pidd*<sup>-/-</sup> and  $E\mu$ -Myc/*Casp2*<sup>-/-</sup> mice and put in culture to assess apoptosis over time by flow cytometric analysis. With the exception of increased apoptosis due to *c-Myc* overexpression, comparable cell death rates were observed across genotypes, indicating that the PIDDo-some does not regulate *c-Myc*-induced apoptosis, at least not in premalignant B cells (Figure 4b). Similarly, immediate assessment of Annexin V/propidium iodide (PI)-positive B cells after organ harvest failed to reveal genotype-dependent differences in *in-situ* apoptosis rates (data not shown). Together, our results exclude a prominent role for impaired apoptosis in the deregulated tumor formation observed in PIDDo-some-deficient mice, pointing toward possible deficits in cell-cycle control or senescence triggered by oncogenic *c-Myc*. Therefore, we investigated the impact of *Pidd* or *Caspase-2* deficiency on proliferation in premalignant mice by *in-vivo* Bromodeoxyuridine (BrdU)-labeling experiments. However, we failed to detect significant differences in the percentage of cycling premalignant B-cell subsets in the absence or presence of the PIDDo-some (Figure 4c), indicating that proliferation is not impaired by the loss of *Caspase-2* or *Pidd* in non-transformed B cells.

As the PIDDo-some has been implicated in DNA-repair processes, we monitored changes in markers of this response, that is,  $\gamma$ H2AX and p53 binding protein 1 (53BP-1), by employing immunofluorescence analysis on FACS-sorted premalignant mature (CD19<sup>+</sup>IgM<sup>+</sup>) splenic B cells from PIDDo-some-defective  $E\mu$ -Myc transgenic mice. Again, we noted no significant difference regarding the amount of DNA damage, as indicated by  $\gamma$ H2AX foci formation, or repair capacity, quantified by counting the number of p53BP-1 containing repair foci across genotypes (Figure 4d). These data suggest

that the DNA-damage response to oncogenic stress is largely functional in PIDDo-some-defective mice.

**Loss of the PIDDo-some associates with impaired M-phase progression in tumor cells.** As we failed to observe relevant changes in PIDDo-some-defective pre-malignant mice, we turned our focus back on diseased mice. Interestingly, *Pidd*-deficient tumors showed an increase in the percentage of cells in G2/M phase compared with wt  $E\mu$ -Myc lymphomas (mean 23±6.6% versus 12±1.1% in G2/M), an effect also noted, albeit less pronounced, in the absence of Caspase-2 (mean 18.3±1.8%; Figure 5a). Staining of the mitotic marker phospho-histone H3 (pH3) revealed a significantly higher percentage of lymphoma cells in mitosis in *Pidd*-deficient tumor samples ( $P=0.0004$ ), and a less pronounced, but still statistically significant elevation ( $P=0.028$ ) was also observed in *Caspase-2*-deficient samples (Figure 5b), a result fitting our cell-cycle analysis. This suggests that cell-cycle progression is impaired in both  $E\mu$ -Myc/*Pidd*<sup>-/-</sup> and  $E\mu$ -Myc/*Casp2*<sup>-/-</sup> tumors and transformed cells may either enter mitosis in increased numbers and/or have problems to exit from mitosis.

Previous reports suggested that Caspase-2 can limit transformation by silencing expression of the chromosome passenger protein Survivin, a protein highly expressed in proliferating (tumor) cells, with putative albeit disputed anti-apoptotic potential.<sup>28</sup> Therefore, we tested a number of IgM<sup>+</sup> tumor samples derived from  $E\mu$ -Myc,  $E\mu$ -Myc/*Pidd*<sup>-/-</sup> and  $E\mu$ -Myc/*Casp2*<sup>-/-</sup> mice for their Survivin protein levels but failed to observe consistent differences. The level of Caspase-2 was comparable in tumors derived from  $E\mu$ -Myc and  $E\mu$ -Myc/*Pidd*<sup>-/-</sup> mice (Figure 5c) and cleaved fragments of Caspase-2 indicative for processing or activation were not detected in this analysis.

To determine a potential contribution of oncogene-induced senescence to delayed tumor onset in  $E\mu$ -Myc/*Pidd*<sup>-/-</sup> mice, we tested lymphoma samples for the presence of lysine-9 methylation of histone H3 by western blotting (Figure 5c), as well as for the expression of the senescence-associated CDK inhibitors p16<sup>ink4a</sup> and p21 by immunofluorescence and/or qRT-PCR. Of note, p21 mRNA levels actually appeared decreased in tumors lacking Caspase-2. However, none of the other markers provided convincing evidence for deregulated senescence capacity in PIDDo-some-deficient cells that may have explained the differences in tumor onset (Figure 2a). Finally, we also quantified serum levels of TGF $\beta$  in premalignant and diseased mice, as this cytokine appears to be a critical non-cell autonomous inducer of senescence, released by macrophages after engulfing apoptotic lymphoma cells.<sup>29</sup> Next to the fact that we observed increased levels of this cytokine in diseased mice we failed to observe statistically significant differences across genotypes (Supplementary Figure 2C). However, variation between individual animals was rather high.

Finally, as PIDDo-some was reported to be involved in NF- $\kappa$ B activation via complex formation together with RIP-1 kinase and NEMO/IKK $\gamma$ <sup>30</sup> and it was recently published that persisting DNA damage can promote secretion of cytokines like tumor necrosis factor  $\alpha$  (TNF $\alpha$ ), interleukin-6 (IL-6) or IL-8<sup>31</sup> that may contribute to generate a pro-inflammatory tumor

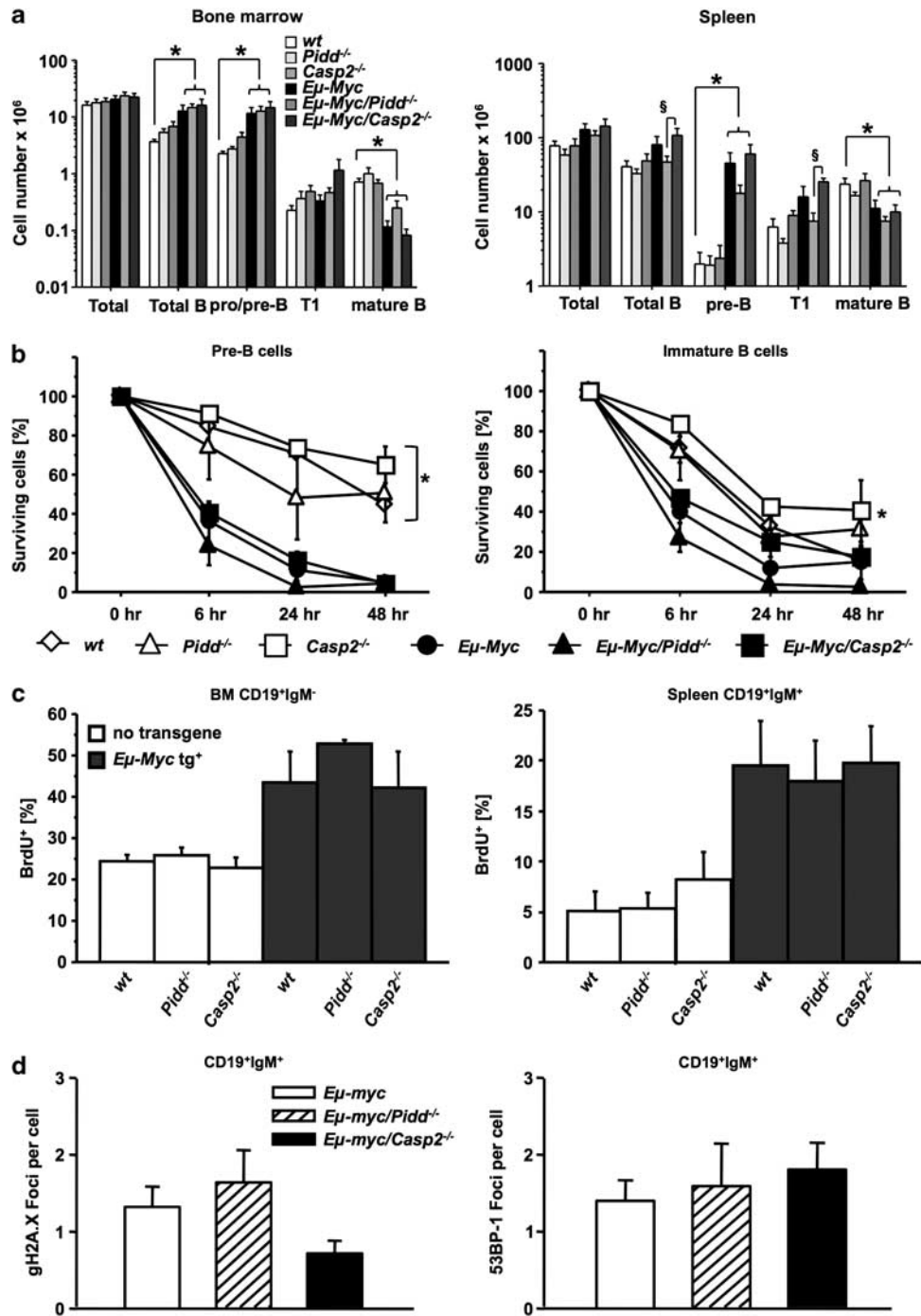


**Figure 4** Normal cell death and proliferation rates in PIDDosome-defective premalignant B cells. (a) Distribution of B-cell subsets in bone marrow, or spleens of mice of the indicated genotypes. Single-cell suspensions derived from premalignant animals 5 weeks of age were counted, stained for different B-cell markers and analyzed by flow cytometry. Data are represented as means of  $n > 4$  animals/genotype  $\pm$  S.E.M. \* $P < 0.05$  compared with *Eμ-Myc* controls,  $^{\S}P < 0.05$  compared with *Eμ-Myc/Casp2*<sup>-/-</sup> mice. (b) Sorted pre-B cells from the bone marrow (CD19<sup>+</sup>IgM<sup>-</sup>CD43<sup>-</sup>), immature B cells (IgM<sup>+</sup>IgD<sup>low</sup>) from the spleens of mice of the indicated genotypes were cultured for 0, 6, 24 and 48 h cells and cell survival in CD19<sup>+</sup> B cells was monitored by Annexin V/PI staining and flow cytometric analysis. Data points represent mean values  $\pm$  S.E.M. from  $n > 3$  cell mice/genotypes. \* $P < 0.05$  all *Eμ-myc* versus all non-transgenic genotypes (ANOVA and Student–Newman–Keuls test). (c) BrdU incorporation was determined in CD19<sup>+</sup>IgM<sup>-</sup> pro/pre-B cells isolated from bone marrow (left) and mature CD19<sup>+</sup>IgM<sup>+</sup> B cells isolated from spleen (right) from indicated genotypes (5 weeks old). Data are mean values  $\pm$  S.E.M. from  $n > 4$  mice/genotypes. (d) Mature B cells (CD19<sup>+</sup>IgM<sup>+</sup>), sorted from spleens derived from premalignant mice of the indicated genotypes, were stained for  $\gamma$ H2AX or 53BP-1 and foci/cells is depicted as bar graphs of mean values  $\pm$  S.E.M. of  $n > 3$  preparations from individual animals

promoting environment, we also quantified these cytokines in serum samples from premalignant and malignant mice. However, levels of TNF $\alpha$ , IL-6 and the mouse ortholog of

human IL-8, MIP-2, were not significantly altered in sera of *Eμ-Myc* mice lacking the PIDDosome but this issue deserves a more detailed follow-up (Supplementary Figure S3).

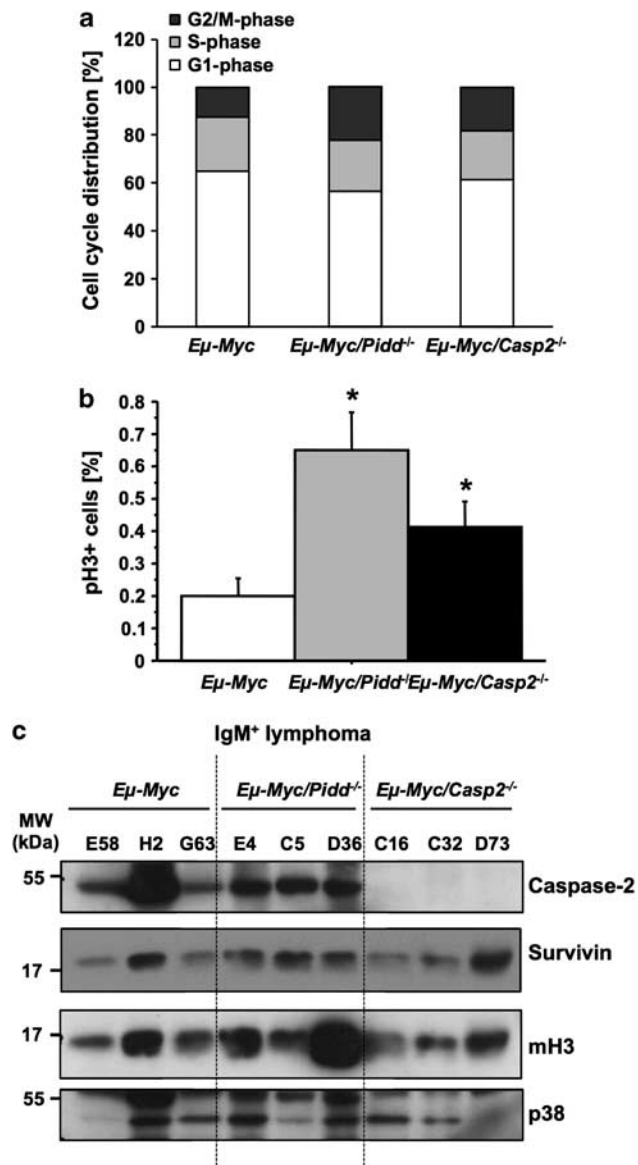


**Figure 5** Lack of *Pidd* or *Caspase-2* leads to a deregulation of cell cycle in *Eμ-Myc* tumors. (a) Cell cycle-distribution is depicted with G1 phase (white), S phase (light gray) and G2/M phase (dark gray) in tumor cells freshly isolated from *Eμ-Myc* ( $n=23$ ), *Eμ-Myc/Pidd<sup>-/-</sup>* ( $n=8$ ) and *Eμ-Myc/Casp2<sup>-/-</sup>* ( $n=13$ ). (b) Tumor cells of wt *Eμ-Myc* ( $n=17$ ), *Eμ-Myc/Pidd<sup>-/-</sup>* ( $n=8$ ) and *Eμ-Myc/Casp2<sup>-/-</sup>* ( $n=13$ ) were co-stained for mitosis-marker pH3 and PI. Bars represent percentages of pH3-positive cells  $\pm$  S.E.M. \* $P < 0.05$ . (c) Representative western blot analysis quantifying Caspase-2, Survivin or Lys<sup>9</sup> pan-methyl H3 (mH3) levels in IgM<sup>+</sup> tumors derived from *Eμ-Myc*, *Eμ-Myc/Pidd<sup>-/-</sup>* and *Eμ-Myc/Casp2<sup>-/-</sup>*. Detection of p38 MAPK served as a loading control

Together these data suggest that B-cell lymphomas from *Eμ-Myc/Pidd<sup>-/-</sup>* mice develop and manifest with a significant delay that is not directly linked to an increased rate of oncogene-driven cellular senescence or defective inflammatory responses but may associate with deregulated M-phase progression, while those lacking Caspase-2 show a trend toward reduced *p21* mRNA levels. Whether any of these alterations is causal for the phenotypes observed remains to be determined.

**Normal cell death responses in PIDDosome-deficient tumor cells.** Tumors derived from wt *Eμ-Myc*, *Eμ-Myc/Pidd<sup>-/-</sup>* and *Eμ-Myc/Casp2<sup>-/-</sup>* mice showed comparable levels of apoptotic cells *in situ* and tumor cells died equally fast, when put in culture without further treatment (Figure 6 and data not shown). Similarly, treatment of primary lymphoma cells wt for p53 according to our western blot analysis with a number of different DNA-damaging agents, including Etoposide and Doxorubicin, or other anti-neoplastic agents reported in part to act via Caspase-2 failed to reveal significant differences between wt, *Pidd<sup>-/-</sup>* or Caspase-2-deficient *Eμ-Myc* tumor cells (Figure 6).

**Tumors lacking Caspase-2 display increased dissemination potential.** Having excluded severe defects in apoptosis or DNA repair in PIDDosome-defective *Eμ-Myc* mice, we performed histological analysis of H&E-stained tumor samples to gain possible insight why Caspase-2 and *Pidd*-defective mice behaved so differently in this model. This analysis revealed that there was a higher tumor infiltration rate in cancerous *Eμ-Myc* mice lacking *Caspase-2*, presenting with pulmonary congestion, loss of splenic parenchymatic architecture and visible hematopoiesis, as well as clear perivascular infiltrations in liver (Figures 7a and b and not shown), a phenomenon not seen to such degree in wt or *Pidd*-deficient *Eμ-Myc* transgenic mice. This observation indicates differences in the migratory potential of tumors lacking *Caspase-2*, or a more permissive tumor microenvironment in Caspase-2-deficient mice allowing B-cell tumors lacking this protease to behave more aggressively, contributing to the reduced disease-free survival. Preliminary data on transplantation experiments suggest that tumors derived from *Eμ-Myc* mice do not arise faster when transplanted into Caspase-2-deficient recipients, indicating that the higher dissemination rate observed in *Eμ-Myc/Casp2<sup>-/-</sup>* mice is most likely not due to a more permissive environment in Caspase-2-deficient soma (Supplementary Figure S4).

## Discussion

The PIDDosome has been implicated in two fundamental, but opposing cellular processes, both being of major importance to limit tumorigenesis, that is, apoptosis and DNA repair. Based on the study from Ho *et al.*,<sup>19</sup> showing a tumor suppressor function for Caspase-2 and correlative findings in human cancer, the role of the PIDDosome was investigated in different tumor models in more detail. Surprisingly, the PIDDosome had no impact on development of radiation-induced thymic lymphomas or chemically induced fibrosarcomas arguing against a critical role of the PIDDosome in suppressing DNA damage-driven apoptosis and related tumorigenesis (Figure 1). In contrast, however, it had a strong influence on the development of *c-Myc*-driven B-cell lymphomas, as loss of *Caspase-2* accelerated disease onset, as previously described,<sup>19</sup> while, surprisingly, loss of *Pidd* delayed disease in *Eμ-Myc* transgenic mice (Figure 2).

As the mechanism behind the tumor suppressor function of Caspase-2 resistance to oncogene-driven apoptosis was proposed, based mainly on studies using E1A/Ras-

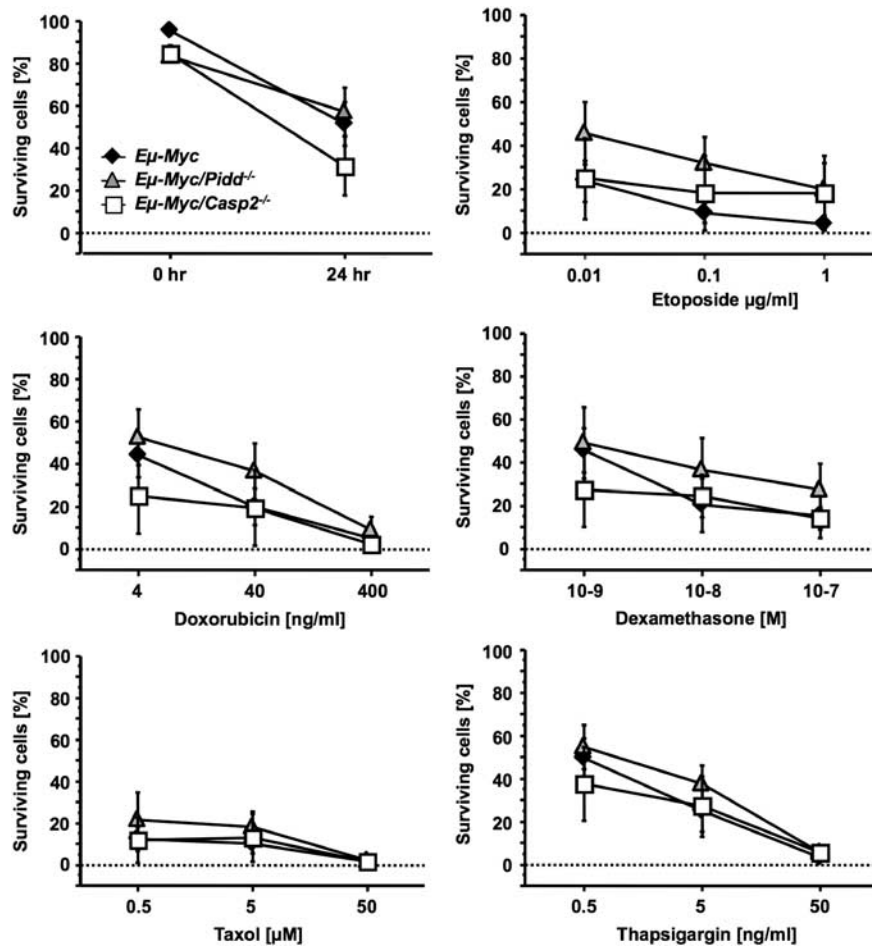


**Figure 6** The PIDDosome is dispensable for drug-induced apoptosis in *Eμ-Myc* lymphomas. Freshly isolated tumor cells from indicated genotypes were cultivated on irradiated Bcl-2 overexpressing NIH-3T3 feeder cells and stimulated with graded doses of different drugs for 24 h. Apoptotic cell death was investigated using Annexin V/7-AAD in combination with anti-CD19 mAb and flow cytometric analysis. Data points represent means of  $n > 3$  tumor samples/genotype  $\pm$  S.E.M.

transformed MEF *in-vitro* and xeno-transplant studies using such MEF. A direct impact of Caspase-2 deficiency on *c-Myc*-driven cell death or proliferation of B cells was not investigated in this study.<sup>19</sup> Our analysis of these parameters demonstrated comparable cell death rates in *c-Myc* overexpressing premalignant B cells proficient or deficient for *Caspase-2* or *Pidd*, arguing against a general resistance of PIDDosome-deficient cells to oncogene-driven cell death. This response may be critical only in response to H-Ras hyperactivation. In contrast to Ho *et al.*, we also failed to observe drug-resistance phenotypes in the Caspase-2-deficient lymphomas studied *in vitro* (Figure 6), observations in line with our studies on primary lymphocytes and MEF from PIDDosome-defective mice.<sup>12,13</sup> The reason for this inconsistency is unclear, but differences in the experimental set-up, such as the use of tumor cells of defined immunophenotype and/or p53 status as well as feeder cells in our study may contribute.

Since mediation of *c-Myc*-driven apoptosis is apparently not the key mechanism behind the tumor suppressor function of Caspase-2 one might speculate whether the proteolytic activity of Caspase-2 itself has an important role. Caspase-2 may act simply as a scaffold for other proteins exerting anti-oncogenic properties. In our study, we observed similar levels

of Caspase-2 protein in wt and *Pidd*-deficient tumors and so far found no evidence for activation of Caspase-2 under conditions of aberrant expression of *c-Myc*.

In line with Ho *et al.*,<sup>19</sup> we also noted a trend to lower mRNA levels of the p53 target *p21* in Caspase-2-deficient tumors. However, our initial analysis on *Eμ-Myc* mice lacking *p21* failed to provide evidence that loss of this CDK inhibitor accelerates onset of lymphomagenesis in this disease model (AN and RJ, unpublished), questioning the importance of this observation. Also, we were unable to confirm these findings at the protein level (Supplementary Figure S2 and data not shown) and data from transplantation experiments comparing the growth of wt and Caspase-2-defective tumors failed to reveal reproducible differences between genotypes (Supplementary Figure S4). Hence, we conclude that neither increased cell death resistance nor increased rates of proliferation account for the observed acceleration of B-cell lymphomagenesis in *Casp2<sup>-/-</sup>* mice. Of note, our histopathological data confirmed a comparable mitotic index between wt and Caspase-2-defective lymphomas (data not shown) but revealed that loss of *Casp2* leads to a more aggressive type of B-cell lymphoma, reflected in a higher infiltration rate of non-lymphoid organs and higher splenic



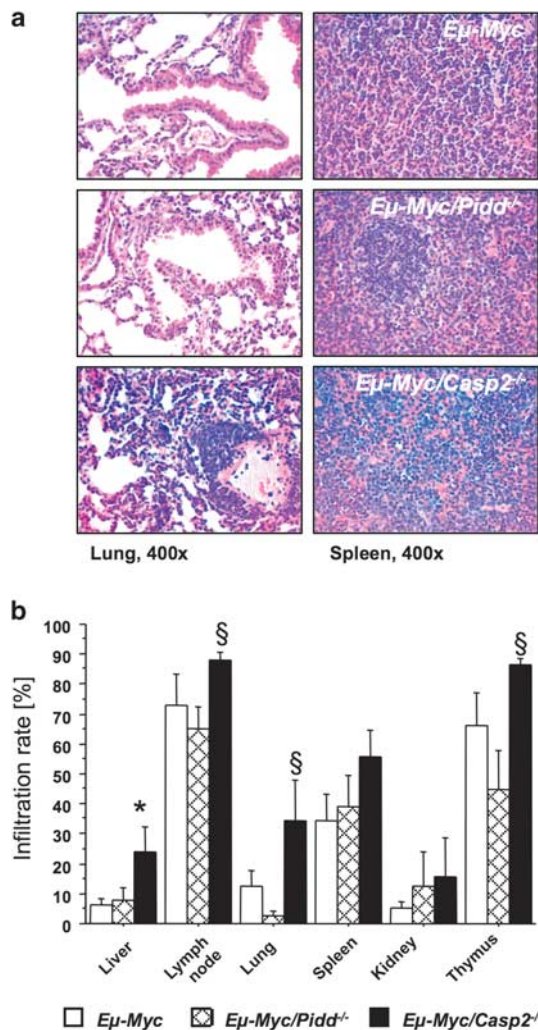


**Figure 7** Loss of *Caspase-2* promotes dissemination of *Eμ-Myc* lymphomas. (a) Representative images of H&E-stained sections from lung (left panel) and spleen (right panel) from mice of the indicated genotypes showing tumor manifestation ( $\times 400$  magnification). (b) Percentage of tumor infiltrated area in indicated organs and genotypes quantified from H&E-stained sections of  $n > 6$  mice per genotype. Data are represented as mean values  $\pm$  S.E.M. \* $\S$ Indicate significant difference with a  $P$ -value of  $< 0.05$  comparing *Eμ-Myc/Casp2*<sup>-/-</sup> with *Eμ-Myc* or *Eμ-Myc/Pidd*<sup>+/-</sup> mice, respectively

weight (Figure 7; Supplementary Figure S1B). This observation points toward a possible role for Caspase-2 in limiting cell migration and/or metastasis potential. Noteworthy here, a recent study describes H-Ras-dependent downregulation of Caspase-2 and subsequent resistance to anoikis in intestinal epithelial cells as a means that facilitates Ras-induced transformation.<sup>32</sup> This observation may in part also explain in part the findings by Ho *et al.*<sup>19</sup> made in E1A/Ras-transformed MEF and xeno-transplants, as well as our observation on increased organ infiltration, but clearly requires experimental evaluation. Finally, the phenotype of Caspase-2-defective *Eμ-Myc* mice is most likely independent of p53, since Caspase-2-deficient lymphomas show a decreased rate of p53 inactivation, suggesting that it acts in a parallel tumor suppressor pathway. Whether Caspase-2-deficient tumors

show increased frequency of Mdm2 overexpression or ARF loss remains to be analyzed.

To our surprise and in contrast to Caspase-2-deficient mice, *Eμ-Myc/pidd*<sup>-/-</sup> mice developed lymphomas at a significantly later time point, assigning it an oncogenic role in B-cell lymphomagenesis. The increased proliferative rate caused by *c-Myc* overexpression is initially balanced by massive apoptosis. Of note, knockdown of PIDD has been proposed to sensitize cells to death upon DNA damage triggered by UV<sup>33</sup> or doxorubicin.<sup>34</sup> In contrast, its overexpression associated with growth arrest in K-Ras<sup>G12D</sup> transformed murine lung carcinomas and human lung cancer cell lines, an effect proposed to be due to improved p53 stability thereby enforcing p21 expression,<sup>34</sup> providing a possible explanation for the delayed tumor formation we observed. However, although we noted a minor reduction in B-cell progenitors in the spleens of *Eμ-Myc* mice lacking *Pidd*, we failed to observe increased spontaneous cell death in premalignant B cells or reduced proliferation, as monitored by BrdU incorporation. Also, level of *p21* mRNA in *Pidd*-defective lymphomas was not different to those in wt tumors, while M-phase progression seemed to be impaired despite this lack of difference. PIDD-deficient lymphomas also responded normally to DNA damaging agents (Figure 6). Together, this indicates that the role of *Pidd* might differ between premalignant and tumor cells and cell type-specific differences need to be taken into account.

Together, our results indicate that Caspase-2 does not limit *c-Myc*-driven transformation by mediating apoptosis or limiting cell-cycle progression in premalignant or malignant cells, but leads to a more aggressive tumor phenotype, indicated by the enhanced dissemination into non-lymphoid organs that associates with the reduced lifespan in these mice. Hence, investigations into a possible role of Caspase-2 in cell migration and anoikis, but also genomic stability, appear warranted. Furthermore, *Pidd* seems to have no impact on limiting cell-cycle progression or cell death in premalignant cells but affects mitosis regulation in *c-Myc* transformed tumor cells, leading to delayed onset of tumorigenesis by a yet to be defined molecular mechanism.

#### Materials and Methods

**Mice.** All animal experiments were performed in accordance with the Austrian legislation (BGBl. Nr. 501/1988 i.d.F. 162/2005, # BMWF-66.011/0137-11/10b/2009). The generation and genotyping of the *Pidd*<sup>-/-</sup>, *Casp2*<sup>-/-</sup>, *Bid*<sup>-/-</sup>, *Trail*<sup>-/-</sup>, *p53*<sup>-/-</sup> and *Eμ-Myc* transgenic mice have been described.<sup>12,35</sup> All mice used were maintained on an inbred C57BL/6 genetic background.

**Tumorigenesis induced by DNA damage.** Mice were exposed to whole body irradiation to four weekly doses of  $\gamma$ -irradiation with 1.75 Gy in a linear accelerator starting at the age of 4 weeks. To induce fibrosarcomas, mice were injected once *i.m.* with 1 mg of 3-MC (dissolved in 200  $\mu$ l sesame oil/mouse; Sigma, Vienna, Austria). As a control, mice were injected with vehicle alone.

**Cell culture and reagents.** FACS-sorted pre-B, immature and mature IgM<sup>+</sup> B cells were cultured in DMEM (PAA) supplemented with 10% FCS (PAA; Linz, Austria), 250  $\mu$ M L-glutamine (Gibco, Life Technologies, Vienna, Austria), streptomycin/penicillin (Sigma) and 50  $\mu$ M beta-2-mercaptoethanol (Sigma). Isolated lymphoma cells were cultured on supporting irradiated NIH-3T3 cells overexpressing Bcl-2. Source/concentrations of reagents are Etoposide (0.01–1  $\mu$ g/ml), Dexamethasone ( $10^{-9}$ – $10^{-7}$ ), Paclitaxel (0.5–50  $\mu$ M), Thapsigargin (0.5–50 ng/ml) and Doxorubicin (4–400 ng/ml) (all from Sigma).

**Histopathology.** Tissues from moribund mice were embedded in paraffin and sections (10  $\mu$ m) were H&E stained. Images were taken using a NIKON Eclipse E800 bright field microscope (Vienna, Austria).

**Flow cytometric analysis and cell sorting.** The monoclonal antibodies used, and their specificities, are as follows: RA3-6B2, anti-B220; R2/60, anti-CD43; II/41, anti-IgM; 11/26C, anti-IgD; MB19-1, anti-CD19; 53-7.3, anti-CD5; GK1.5, anti-CD4; H57-597, anti-TCR $\beta$  (all from eBioscience, Vienna, Austria); 53-6.7, anti-CD8; (all from BD Pharmingen, San Diego, CA, USA) and B3B4, anti-CD23; 7E9, anti-CD21 (Biologend, Fell, Germany). Biotinylated antibodies were detected using streptavidin-RPE (DAKO, Vienna, Austria) or streptavidin-PE-Cy7 (BD Pharmingen). Pre/pro B cells (B220<sup>+</sup>IgM<sup>-</sup>) were sorted from the bone marrow stained for B220 and IgM, while immature (IgM<sup>+</sup>IgD<sup>low</sup>) and mature (IgM<sup>+</sup>IgD<sup>high</sup>) B cells were sorted from the spleen using a FACS<sup>Vantage</sup> cell sorter (Becton Dickinson, Heidelberg, Germany).

**Immunoblotting.** Membranes were probed with rat anti-p19/ARF (5-C3-1) (Santa Cruz Biotechnology, Szabo-Scandic, Vienna, Austria), Caspase-2 (11B6) (Alexis, Vienna, Austria), mouse anti-p53 antiserum (1C12) and pan-methyl Histone H3 (Lys9), Survivin (71G4B7) or p38 MAPK (8690) (all from Cell Signaling, New England Biolabs, Frankfurt, Germany). Equal loading of proteins was confirmed by probing filters with antibodies specific for GAPDH (Sigma). Horseradish peroxidase-conjugated sheep anti-rat Ig antibodies (Jackson Research, Vienna, Austria), goat anti-rabbit or rabbit anti-mouse antibodies (DAKO) served as secondary reagents and the enhanced chemiluminescence (ECL; Amersham, Freiburg, Germany) system was used for detection.

**Cell-cycle analysis.** Cell-cycle analysis was performed by ethanol fixation (70% in PBS) of the lymphoma cells and PI staining (40  $\mu$ g/ml; Sigma). The percentage of cells in M phase was evaluated by combined PI and anti-phospho-H3<sup>Ser10</sup> staining (Cell Signaling) of ethanol fixed lymphoma cells. Samples were analyzed in a FACScan flow cytometer and data were evaluated using WinMDI2.8 freeware.

**BrdU incorporation.** *In-vivo* rates of B-cell proliferation was determined by BrdU incorporation using an APC-labeled anti-BrdU mAb as described by the manufacturer (BrdU-APC flow kit; BD Bioscience, Vienna, Austria). Briefly, healthy animals at the age of 5 weeks were injected with 1 mg BrdU/mouse (in 200  $\mu$ l saline) and killed after 4 h. B cells were stained with fluorochrome-conjugated antibodies staining IgM or CD19 and were analyzed by FACScan (Becton Dickinson).

**Cell viability assay.** The percentage of viable cells in culture was determined by staining cell suspensions with 1  $\mu$ g/ml 7-AAD (Sigma) plus FITC-coupled Annexin V (Becton Dickinson). The samples were analyzed in a FACScan (Becton Dickinson).

**Immunofluorescence staining.** To monitor 53BP-1 and  $\gamma$ H2AX foci, sorted immature and mature B cells from *E $\mu$ -Myc*, *E $\mu$ -Myc/Pidd<sup>-/-</sup>* and *E $\mu$ -Myc/Casp2<sup>-/-</sup>* mice were stained as described elsewhere (Viale et al., 2009).<sup>36</sup> Pictures were taken with a Leica SP5 confocal laser-scanning microscope (Vienna, Austria) equipped with a  $\times$  63 glycerol immersion objective, and images were analyzed using CellProfiler freeware (Broad Institute, Harvard, MA, USA).

**Statistical analysis.** Estimation of statistical differences between groups was carried out using the unpaired Student's *t*-test or ANOVA analysis with Student–Newman–Keuls as *post hoc* test, where appropriate. Comparison of tumor onset was performed using a log-rank test and the  $\chi^2$ -test (Fisher's exact) was used for comparison of frequency distributions. *P*-values of <0.05 were considered to indicate statistically significant differences.

### Conflict of Interest

The authors declare no conflict of interest.

**Acknowledgements.** We thank K Rossi and B Rieder for animal husbandry; C Soratroi, R Pfeilschifter, I Gaggli and I Brösch for excellent technical assistance; P Lukas and his team (LINAC1-4) for enabling irradiation of mice (Center of Nuclear Medicine and Radiotherapy, University Medical Center of Innsbruck); G Böck for cell sorting; G Baier and N Herman-Kleifer for help with Bioplex analysis; D Vaux for *Casp2<sup>-/-</sup>* and M Serrano for *p53<sup>-/-</sup>* mice. This study was funded by the Austrian Science Fund (FWF; Y212-B12; SFB021), AICR project 06-440 to AV and

the FP06 RTN 'ApopTrain' to AV and FB as well as the Daniel Swarovski Fond (DSF) and the Tyrolean Science Fund (TWF) to CM and the Austrian Krebshilfe-Tirol (CM and GK). RWJ is a Principal Research Fellow of the National Health and Medical Research Council of Australia (NHMRC) and supported by NHMRC Program and Project Grants, the Susan G Komen Breast Cancer Foundation, the Prostate Cancer Foundation of Australia, Cancer Council Victoria, The Leukemia Foundation of Australia, Victorian Breast Cancer Research Consortium, Victorian Cancer Agency and the Australian Rotary Health Foundation.

1. Vakifahmetoglu-Norberg H, Zhivotovsky B. The unpredictable caspase-2: what can it do? *Trends Cell Biol* 2010; **20**: 150–159.
2. Kurokawa M, Kornbluth S. Caspases and kinases in a death grip. *Cell* 2009; **138**: 838–854.
3. Krumschnabel G, Sohm B, Bock F, Manzl C, Villunger A. The enigma of caspase-2: the laymen's view. *Cell Death Diff* 2009; **16**: 195–207.
4. Tinel A, Tschopp J. The PIDDosome, a protein complex implicated in activation of caspase-2 in response to genotoxic stress. *Science* 2004; **304**: 843–846.
5. Sidi S, Sanda T, Kennedy RD, Hagen AT, Jette CA, Hoffmans R et al. Chk1 suppresses a caspase-2 apoptotic response to DNA damage that bypasses p53, Bcl-2, and caspase-3. *Cell* 2008; **133**: 864–877.
6. Olsson M, Vakifahmetoglu H, Abruzzo PM, Hogstrand K, Grandien A, Zhivotovsky B. DISC-mediated activation of caspase-2 in DNA damage-induced apoptosis. *Oncogene* 2009; **28**: 1949–1959.
7. Vakifahmetoglu H, Olsson M, Orrenius S, Zhivotovsky B. Functional connection between p53 and caspase-2 is essential for apoptosis induced by DNA damage. *Oncogene* 2006; **25**: 5683–5692.
8. Castedo M, Perfettini JL, Roumier T, Valent A, Raslova H, Yakushijin K et al. Mitotic catastrophe constitutes a special case of apoptosis whose suppression entails aneuploidy. *Oncogene* 2004; **23**: 4362–4370.
9. Baptiste-Okoh N, Barsotti AM, Prives C. A role for caspase 2 and PIDD in the process of p53-mediated apoptosis. *Proc Natl Acad Sci USA* 2008; **105**: 1937–1942.
10. Lin Y, Ma W, Benchimol S. Pidd, a new death-domain-containing protein, is induced by p53 and promotes apoptosis. *Nat Genet* 2000; **26**: 124–127.
11. Kim IR, Murakami K, Chen NJ, Saibil SD, Matysiak-Zablocki E, Elford AR et al. DNA damage- and stress-induced apoptosis occurs independently of PIDD. *Apoptosis* 2009; **14**: 1039–1049.
12. Manzl C, Krumschnabel G, Bock F, Sohm B, Labi V, Baumgartner F et al. Caspase-2 activation in the absence of PIDDosome formation. *J Cell Biol* 2009; **185**: 291–303.
13. Berube C, Boucher LM, Ma W, Wakeham A, Salmena L, Hakem R et al. Apoptosis caused by p53-induced protein with death domain (PIDD) depends on the death adapter protein RAIDD. *Proc Natl Acad Sci USA* 2005; **102**: 14314–14320.
14. O'Reilly LA, Ekert P, Harvey N, Marsden V, Cullen L, Vaux DL et al. Caspase-2 is not required for thymocyte or neuronal apoptosis even though cleavage of caspase-2 is dependent on both Apaf-1 and caspase-9. *Cell Death Diff* 2002; **9**: 832–841.
15. Bergeron L, Perez GI, Macdonald G, Shi L, Sun Y, Jurisicova A et al. Defects in regulation of apoptosis in caspase-2-deficient mice. *Genes Dev* 1998; **12**: 1304–1314.
16. Marsden VS, Ekert PG, Van Delft M, Vaux DL, Adams JM, Strasser A. Bcl-2-regulated apoptosis and cytochrome c release can occur independently of both caspase-2 and caspase-9. *J Cell Biol* 2004; **165**: 775–780.
17. Kumar S. Caspase 2 in apoptosis, the DNA damage response and tumour suppression: enigma no more? *Nat Rev Cancer* 2009; **9**: 897–903.
18. Bradley G, Tremblay S, Irish J, MacMillan C, Baker G, Gullane P et al. The expression of p53-induced protein with death domain (PIDD) and apoptosis in oral squamous cell carcinoma. *Br J Cancer* 2007; **96**: 1425–1432.
19. Ho LH, Taylor R, Dorstyn L, Cakouros D, Bouillet P, Kumar S. A tumor suppressor function for caspase-2. *Proc Natl Acad Sci USA* 2009; **106**: 5336–5341.
20. Kaplan HS, Brown MB. A quantitative dose-response study of lymphoid-tumor development in irradiated C57 black mice. *J Natl Cancer Inst* 1952; **13**: 185–208.
21. Kemp CJ, Wheldon T, Balmain A. p53-deficient mice are extremely susceptible to radiation-induced tumorigenesis. *Nat Genet* 1994; **8**: 66–69.
22. Garcia-Cao I, Garcia-Cao M, Martin-Caballero J, Criado LM, Klatt P, Flores JM et al. "Super p53" mice exhibit enhanced DNA damage response, are tumor resistant and age normally. *EMBO J* 2002; **21**: 6225–6235.
23. Adams JM, Harris AW, Pinkert CA, Corcoran LM, Alexander WS, Cory S et al. The *c-myc* oncogene driven by immunoglobulin enhancers induces lymphoid malignancy in transgenic mice. *Nature* 1985; **318**: 533–538.
24. Guo Y, Srinivasula SM, Druilhe A, Fernandes-Alnemri T, Alnemri ES. Caspase-2 induces apoptosis by releasing proapoptotic proteins from mitochondria. *J Biol Chem* 2002; **277**: 13430–13437.
25. Shin S, Lee Y, Kim W, Ko H, Choi H, Kim K. Caspase-2 primes cancer cells for TRAIL-mediated apoptosis by processing procaspase-8. *EMBO J* 2005; **24**: 3532–3542.
26. Eischen CM, Weber JD, Roussel MF, Sherr CJ, Cleveland JL. Disruption of the ARF-Mdm2-p53 tumor suppressor pathway in Myc-induced lymphomagenesis. *Genes Dev* 1999; **13**: 2658–2669.

27. Frenzel A, Labi V, Chmielewski W, Ploner C, Geley S, Fiegl H *et al*. Suppression of B-cell lymphomagenesis by the BH3-only proteins Bmf and Bad. *Blood* 2010; **115**: 995–1005.
28. Guha M, Xia F, Raskett CM, Altieri DC. Caspase 2-mediated tumor suppression involves survivin gene silencing. *Oncogene* 2010; **29**: 1280–1292.
29. Reimann M, Lee S, Loddenkemper C, Dorr JR, Tabor V, Aichele P *et al*. Tumor stroma-derived TGF-beta limits myc-driven lymphomagenesis via Suv39h1-dependent senescence. *Cancer Cell* 2010; **17**: 262–272.
30. Janssens S, Tinel A, Lippens S, Tschopp J. PIDD mediates NF-kappaB activation in response to DNA damage. *Cell* 2005; **123**: 1079–1092.
31. Biton S, Ashkenazi A. NEMO and RIP1 control cell fate in response to extensive DNA damage via TNF-alpha feedforward signaling. *Cell* 2011; **145**: 92–103.
32. Yoo BH, Wang Y, Erdogan M, Sasazuki T, Shirasawa S, Corcos L *et al*. Oncogenic ras-induced downregulation of a pro-apoptotic protease caspase-2 is required for malignant transformation of intestinal epithelial cells. *J Biol Chem* 2011; **286**: 38894–38903.
33. Logette E, Schuepbach-Mallepell S, Eckert MJ, Leo XH, Jaccard B, Manzl C *et al*. PIDD orchestrates translesion DNA synthesis in response to UV irradiation. *Cell Death Diff* 2011; **18**: 1036–1045.
34. Oliver TG, Meylan E, Chang GP, Xue W, Burke JR, Humpton TJ *et al*. Caspase-2-mediated cleavage of Mdm2 creates a p53-induced positive feedback loop. *Mol Cell* 2011; **43**: 57–71.
35. Harris AW, Pinkert CA, Crawford M, Langdon WY, Brinster RL, Adams JM. The Em-myc transgenic mouse: a model for high-incidence spontaneous lymphoma and leukemia of early B cells. *J Exp Med* 1988; **167**: 353–371.
36. Viale A, De Franco F, Orleth A, Cambiaghi V, Giuliani V, Bossi D *et al*. Cell-cycle restriction limits DNA damage and maintains self-renewal of leukaemia stem cells. *Nature* 2009; **457**: 51–56.



This work is licensed under the Creative Commons Attribution-NonCommercial-No Derivative Works 3.0 Unported License. To view a copy of this license, visit <http://creativecommons.org/licenses/by-nc-nd/3.0>

Supplementary Information accompanies the paper on Cell Death and Differentiation website (<http://www.nature.com/cdd>)